Bcl-x and Bax Regulate Mouse Primordial Germ Cell Survival and Apoptosis during Embryogenesis

Edmund B. Rucker III, Patricia Dierisseau, Kay-Uwe Wagner, Lisa Garrett, Anthony Wynshaw-Boris*, Jodi A. Flaws, and Lothar Hennighausen

Laboratory of Genetics and Physiology (E.B.R., P.D., K.-U.W., L.H.)
National Institute of Diabetes, Digestive and Kidney Diseases
National Institutes of Health
Bethesda, Maryland 20892

Genetic Disease Research Branch (L.G., A.W.-B.)
National Human Genome Research Institute
National Institutes of Health
Bethesda, Maryland 20892

Department of Epidemiology and Preventive Medicine (J.A.F.)
University of Maryland School of Medicine
Baltimore, Maryland 21201

Restricted germ cell loss through apoptosis is initiated in the fetal gonad around embryonic day 13.5 (E13.5) as part of normal germ cell development. The mechanism of this germ cell attrition is unknown. We show that Bcl-x plays a crucial role in maintaining the survival of mouse germ cells during gonadogenesis. A *bcl-x* hypomorphic mouse was generated through the introduction of a neomycin (*neo*) gene into the promoter of the *bcl-x* gene by homologous recombination. Mice that contained two copies of the hypomorphic allele had severe reproductive defects attributed to compromised germ cell development. Males with two mutant alleles lacked spermatogonia and were sterile; females showed a severely reduced population of primordial and primary follicles and exhibited greatly impaired fertility. Primordial germ cells (PGCs) in *bcl-x* hypomorph mice migrated to the genital ridge by E12.5 but were depleted by E15.5, a time when Bcl-x and Bax were present. Two additional *bcl-x* transcripts were identified in fetal germ cells more than 300 bp upstream of previously reported start sites. Insertion of a *neo* cassette led to a down-regulation of the *bcl-x* gene at E12.5 in the hypomorph. Bax was detected by immunohistochemistry in germ cells from *bcl-x* hypomorph and control testes at E12.5 and E13.5. Bcl-x function was restored, and animals of both genders were fertile after removal of the *neo* selection cassette using Cre-mediated recombination. Alternatively, the loss of Bcl-x function in the hypomorph was corrected by the deletion of both copies of the *bax* gene, resulting in a restoration of germ cell survival. These findings demonstrate that the balance of Bcl-x and Bax control PGC survival and apoptosis. (Molecular Endocrinology 14: 1038–1052, 2000)

0888-8809/00/$3.00/0
Molecular Endocrinology 14(7): 1038–1052

INTRODUCTION

Formation of the mouse fetal gonad begins with the migration of the primordial germ cells (PGCs) from the base of the allantois at embryonic day 8.5 (E8.5) to the genital ridge at E11.5 (1, 2). During this migratory period, the number of PGCs increases from about 100 to more than 3,000 and by E13.5, PGCs number greater than 22,000 in the fetal gonads (3). After the colonization of the gonads, the gonocytes continue to proliferate but also undergo a transient burst of apoptosis around E13.5 (4). The majority of gonocytes in the testes enter mitotic arrest as prospermatogonia by E15.5 (5), whereas the germ cells in the ovaries enter prophase I of meiosis around E13.5 (6). A second round of apoptosis is initiated in the postnatal testis concomitantly with the initiation of spermatogenesis around postnatal day 8 (p8) (7–9) and in the prepubertal ovary between P7 and P14 (4, 10).

Although the loss of rodent PGCs has been attributed to apoptosis as determined by flow cytometry (4), electron microscopy (11), and 3′-end labeling for DNA fragmentation (10), the genetic pathways controlling fetal gonadal development are largely unknown. While c-*kit* and its ligand mast cell growth factor (MGF) have

been shown to control the migration of PGCs to the genital ridge before E12.5 (12, 13), little is known about the molecular mechanisms controlling the survival and restricted apoptosis that occur at subsequent fetal stages. In contrast, members of the Bcl-2 family have been shown to govern postpartum stages of gametogenesis. For example, *bax*-deficient mice exhibit reduced cell death during spermatogenesis and folliculogenesis. In males, this leads to an increase in the number of spermatocytes (14) and in females to an abundance of ovarian follicles in postnatal life (15). Mice deficient in Bcl-w have defective spermatogenesis and spermiogenesis, which results in a Sertoli-cell-only phenotype by 6 months of age (16, 17).

Bcl-x, a protein controlling cell survival, is expressed widely during development (18). Previous studies have shown that mice harboring an inactivated *bcl-x* gene[1] die at E12.5 (19). Therefore, it was not possible to establish the role of Bcl-x in the ontogeny of gonads and other organs at later stages of development. To understand the role of Bcl-x in organ development, it is therefore necessary to inactivate the gene exclusively in specific cell types using the Cre-loxP recombination system (20). Toward this goal, we have used homologous recombination to flank the promoter, exon 1, and the major coding exon 2 of the *bcl-x* gene with loxP sites. This targeted allele contained a loxP flanked (or floxed) *neo* cassette in the *bcl-x* promoter and an additional loxP site in intron 2. Mice that contained two neomycin-tagged targeted alleles (*bcl-x* fl^{neo}/fl^{neo}) had a dramatically attenuated reproductive ability due to down-regulation of the *bcl-x* gene (*i.e.* a hypomorphic allele). The hypomorphic allele of *bcl-x* has allowed us to define its function as a principal cell survival molecule in germ cell development. Selective placement of loxP sites flanking the *neo* cassette facilitated its removal by partial Cre-mediated recombination. Mice obtained by this method contained a floxed *bcl-x* gene *(fl)* with a single loxP site in the promoter and a second loxP site in intron 2. The ablation of the *neo* cassette restored *bcl-x* expression and eliminated the male and female loss-of-germ-cell phenotype.

Because the mechanism behind normal germ cell death was unknown, we have investigated whether a Bcl-x/Bax rheostat might explain the dynamics involved in germ cell survival and death in the fetal gonad. To test this hypothesis, we also have generated mice that contained two copies of the *bcl-x* hypomorph allele and two *bax* null alleles to quantitate surviving germ cells. Our model postulates that the loss of Bcl-x (cell survival factor) during this period of apoptosis would result in a relative increase in the amount of Bax (cell death factor), thereby forcing the germ cells into premature cell death. Concomitant loss of the *bax* alleles should restore the balance of survival and death factors and result in an increase in germ cell numbers.

[1] GenBank accession number AF088904.

RESULTS

Bcl-x fl^{neo}/fl^{neo} Mice Show a Loss of Spermatogonia and Oocytes

As part of the targeting strategy, exons 1 and 2 of the *bcl-x* gene were floxed by loxP sites, and a *neo* gene was introduced into the *bcl-x* promoter (Fig. 1A). Chimeras were generated from embryonic stem cells that were targeted as determined by Southern blot (Fig. 1B) and PCR analysis (Fig. 1C). All homozygous males that carried two targeted alleles (fl^{neo}/fl^{neo} mice) were sterile.

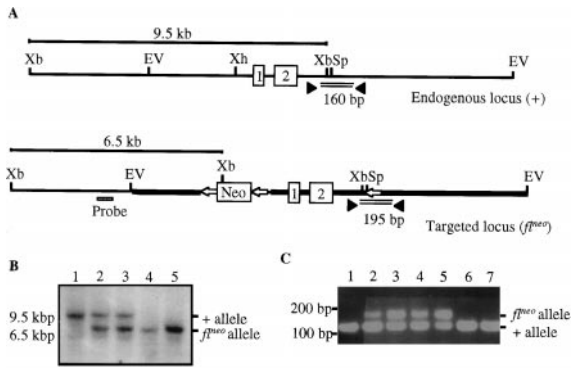

Fig. 1. Generation of fl^{neo} Mice

A, Schematic representation of the *bcl-x* endogenous (+) locus and predicted targeted (fl^{neo}) allele. *Open boxes* represent exons with corresponding exon numbers. The PGK-neo cassette was cloned into the promoter *Xho*I site in the antisense direction. *Open arrows* denote 34-bp loxP sites; PCR primers are represented by *filled triangles* in intron 2. The third loxP site was cloned into the *Spe*I site. Predicted amplification of the intron 2 region with primers should give an endogenous band of approximately 160 bp and a targeted band of 195 bp. The *bold line* shown in the targeted locus represents the *Eco*RV-*Eco*RV region of homology used in the targeting construct. Predicted fragment sizes for the endogenous and targeted alleles from a *Xba*I digest using the shown external probe are 9.5 kb and 6.5 kb, respectively. Restriction enzyme sites shown are *EV, Eco*RV; Sp, *Spe*I; Xb, *Xba*I; Xh, *Xho*I. B, Homologous recombination at the *bcl-x* locus results in the decrease of a 9.5-kb *Xba*I allele to a 6.5-kb allele. A Southern blot was performed from *Xba*I-digested genomic tail DNA from F_2 generation mice using the 5′-external probe as shown in panel A. Wild-type mice (+/+) contain the endogenous 9.5-kb allele, whereas the heterozygous ($fl^{neo}/+$) and homozygous (fl^{neo}/fl^{neo}) *bcl-x* mice contain either one or two targeted alleles of 6.5 kb. Lane 1, control; lanes 2 and 3, heterozygous floxed; lanes 4 and 5, homozygous floxed. C, PCR verifies the presence of the flanking loxP site in targeted ES cells. Genomic DNA from ES cell clones was amplified using above primers to reveal the endogenous and floxed alleles as predicted from panel A. Lanes 1–6 (targeted ES clone) and 7 (nontargeted clone) show the PCR products with the predicted 165-bp and 195-bp bands. Products were subsequently isolated and sequenced for verification. Note that clones 1 and 6 did not contain the loxP site in intron 2, indicating that homologous recombination must have occurred upstream of that site.

Approximately 25% of the females were fertile (n > 20), but they never gave birth to more than three pups. The testes from adult fl^{neo}/fl^{neo} mice were considerably smaller than those of wild-type controls (Fig. 2A). HistoBank accession numbers for all images are shown in Table 1. HistoBank can be accessed at

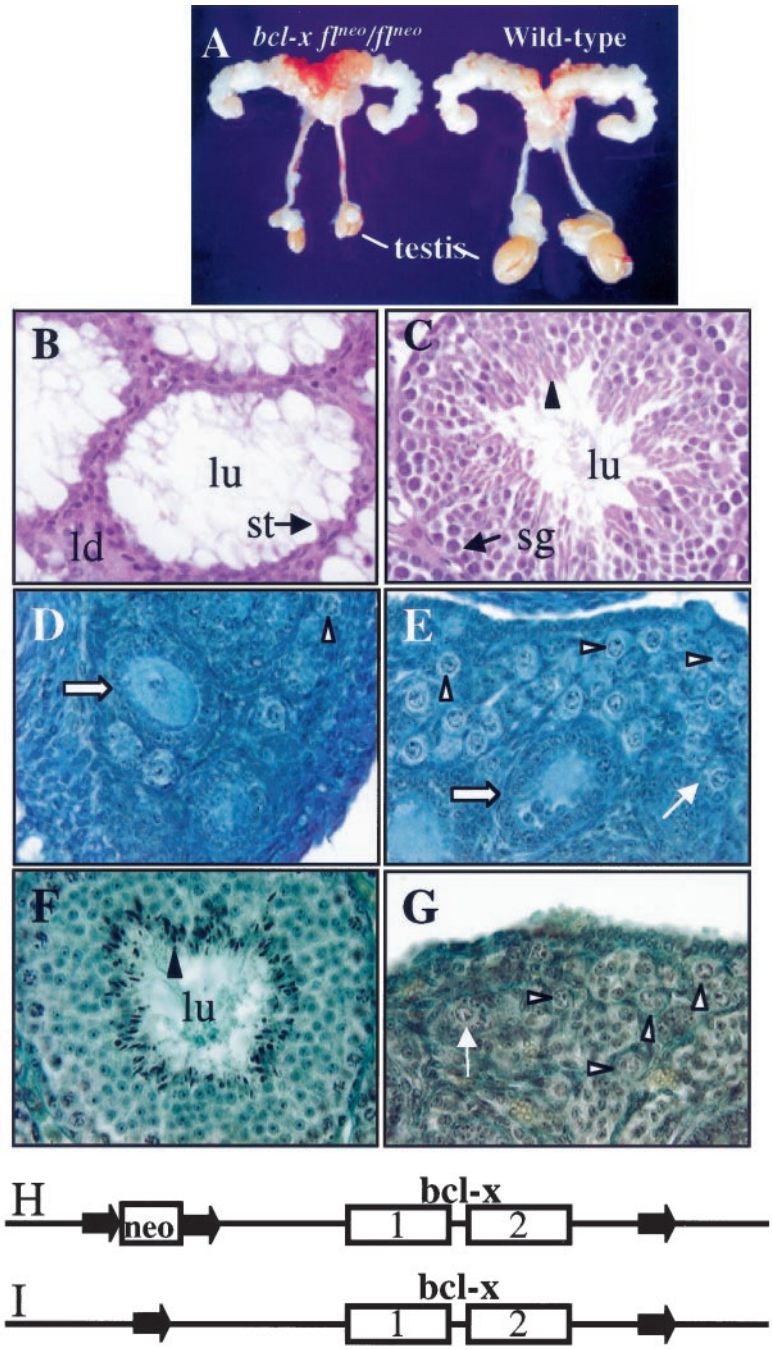

Fig. 2. Reproductive Organs in Wild-Type and fl^{neo}/fl^{neo} Mice

A, Comparison of genital tracts from fl^{neo}/fl^{neo} and wild-type 3.5-month-old males (HistoBank accession numbers 1456, 1457, 1458). Cross-sections of seminiferous tubules of fl^{neo}/fl^{neo} (B) (accession numbers 1342 and 1362) and control (C) (accession number 1363) testes shown in panel A. Ovaries from p9 reveal a decline in primordial follicles in fl^{neo}/fl^{neo} ovaries (D) compared with controls (E). Removal of the *neo* cassette reverted the loss-of-germ-cell phenotype as shown in 2-month-old *fl/fl* testis (F) and ovary (G). H, Schematic representation of the hypomorphic, targeted *bcl-x* locus containing the loxP-flanked *neo* cassette in the promoter. *Block arrows* represent loxP sites. I, Schematic representation of the floxed *bcl-x* locus after removal of the *neo* cassette. *Arrowhead*, Sperm; lu, lumen; sg, spermatogonial cell; st, Sertoli cell; ld, Leydig cell; *white arrowhead*, primordial follicle; *arrow*, primary follicle; *white block arrow*, preantral and early antral stage follicles. Sections in panels B and C were stained by H&E. Sections in panels D, E, F, and G were visualized using Weigert's stain. Original magnification is 0.8× (panel A) and 630× (panels B, C, D, E, F, and G).

http://HistoBank.nih.gov. The small testes size in *fl*^{neo}/*fl*^{neo} mice was due to the absence of spermatogonia, spermatocytes, and spermatids from the seminiferous tubules (Fig. 2B). Seminiferous tubules from control (wild-type or *fl*^{neo}/+) mice contained the expected mixed population of developing germ cells undergoing spermatogenesis (Fig. 2C). The accessory glands and seminal vesicles from *fl*^{neo}/*fl*^{neo} mice did not reveal any overt morphological phenotypic differences. At p9, testes did not have spermatogonia as determined by germ cell nuclear antigen immunohistochemistry (GCNA IHC) (data not shown).

At p9, *fl*^{neo}/*fl*^{neo} ovaries (Fig. 2D) contained 94% fewer primordial follicles than control ovaries (Fig. 2E). Normal ovaries at p9 consisted of primordial follicles, each of which contained an intact oocyte surrounded by a single layer of morphologically normal granulosa cells. The number of primordial follicles in *fl*^{neo}/*fl*^{neo} ovaries decreased from p1 (33.9%) to p19 (6.4%) compared with follicle counts from normal ovaries. At p19 and at 3 months, follicle counts from control and *fl*^{neo}/*fl*^{neo} ovaries were even more distinct from each other (Fig. 3, A and B). Although the primordial follicle counts relative to controls did not change in *fl*^{neo}/*fl*^{neo} ovaries at p19 and 3 months (6.4% *vs.* 5%), there was a decline in the populations of primary (32.7% *vs.* 14.5%) and preantral staged follicles (73.1% *vs.* 23.4%) with advancing age (Fig. 3).

To distinguish whether the observed phenotype was the result of structural rearrangements of the *bcl-x* locus after targeting or a hypomorphic allele, we modified the targeted allele (Fig. 2H) by breeding *fl*^{neo}/+ mice into the *EIIaCre* line (21). *Bcl-x fl*^{neo}/+*; EIIaCre* transgenic mice exhibiting mosaic deletion patterns (*i.e.* incomplete Cre-mediated deletion) and were assayed by PCR for the deletion of the neo cassette (Fig. 2I) and then backcrossed into wild-type mice to remove the Cre transgene. Additionally, *bcl-x* null alleles (−), which lacked exons 1 and 2, were also generated as described in *Materials and Methods*. The loss-of-germ cell phenotype was reverted upon removal of the *neo* gene (Fig. 2, F and G and Fig. 3A). All *fl/fl* (no neo; Fig. 2F) and *fl*/− males (n > 20) were fertile with active spermatogenesis occurring in the seminiferous tubules. Similarly, *fl/fl* and *fl*/− females were fertile (n>20) and had normal litter sizes and a normal distribution of follicles (Figs. 2G and 3A).

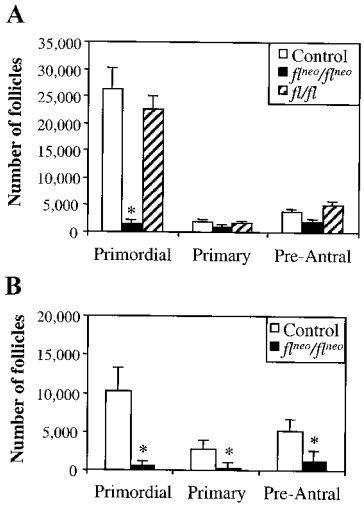

Fig. 3. Graphic Depiction of Follicle Numbers in *bcl-x fl*^{neo}/fl^{neo} *and Wild-Type Ovaries at p19 (A) and 3 Months (B)*

Data represent the mean ± SEM. For p19, n = 3 for control, and n = 4 for *fl/fl* and *fl*^{neo}/*fl*^{neo}. For primordial follicles at p19, $P < 0.002$ for *fl*^{neo}/*fl*^{neo}. For 3 months n = 3 for *fl/fl*, n = 5 for *fl*^{neo}/*fl*^{neo}, n = 7 for control. $P = 0.001$ for primordial follicles; $P = 0.14$ for primary follicles; $P = 0.005$ for antral staged follicles.

Germ Cell Depletion in *fl*^{neo}/*fl*^{neo} Embryos

Hematoxylin-eosin (H&E) staining was used to identify whether germ cells were lost during migration or depleted during development. Analyses of fetal testes (E12.5–E14.5) from *fl*^{neo}/*fl*^{neo} embryos established that although the germ cells had entered the developing genital ridge, there was a decline in gonocytes between E12.5 (Fig. 4, A and G) and E13.5 (Fig. 4, B and H). By E14.5, the loss of spermatogonia was reflected by the formation of a lumen in the developing testis cords (Fig. 4, C and I). GCNA antibodies can be used for germ cell detection from E11.5 to the diplotene/dictyate stage of the first meiotic division (22). In males, GCNA is found in spermatogonia, spermatocytes, and round spermatids; in females, it is present until oocytes arrest at the dictyate stage and gain a layer of granulosa cells (22). GCNA IHC confirmed the decrease in germ cell numbers between E12.5 and E14.5 (Fig. 4, D–F and J–L). Morphometric analyses revealed that *fl*^{neo}/*fl*^{neo} testis contained similar numbers of germ cells as wild-type controls at E12.5, and that the numbers decreased to 68% of controls at E13.5 and 15% at E14.5 (Fig. 5).

Whole-mount alkaline phosphatase (AP) staining and GCNA IHC of *fl*^{neo}/*fl*^{neo} ovaries also showed a decrease in germ cell numbers from E13.5–E15.5 (Fig. 6). Classically, AP reactivity has been used for primordial germ cell detection from E8.5–E15.5 (23). AP staining was decreased in E12.5 and E13.5 *fl*^{neo}/*fl*^{neo} ovaries (Fig. 6, B and D) compared with wild-type controls (Fig. 6, A and C). GCNA IHC on E14.5 and E15.5 wild-type ovaries (Fig. 6, E and G) showed normal germ cells within the developing organ. However, E14.5 *fl*^{neo}/*fl*^{neo} ovaries contained germ cells with fragmented nuclei (Fig. 6F), and by E15.5 the number of germ cells present had greatly diminished (Fig. 6H). Histological evaluation of embryonic ovaries indicated that *fl*^{neo}/*fl*^{neo} ovaries did not contain fewer gonocytes at E12.5 than wild-type controls. However, by E13.5, the number of germ cells had decreased to 42% (not shown). Apoptotic germ cells were characterized by condensed, darkly staining pyknotic nuclei that often appear fragmented. E13.5 testes showed higher levels of apoptotic germ cells in *fl*^{neo}/*fl*^{neo} (18.6% ± 6.7;

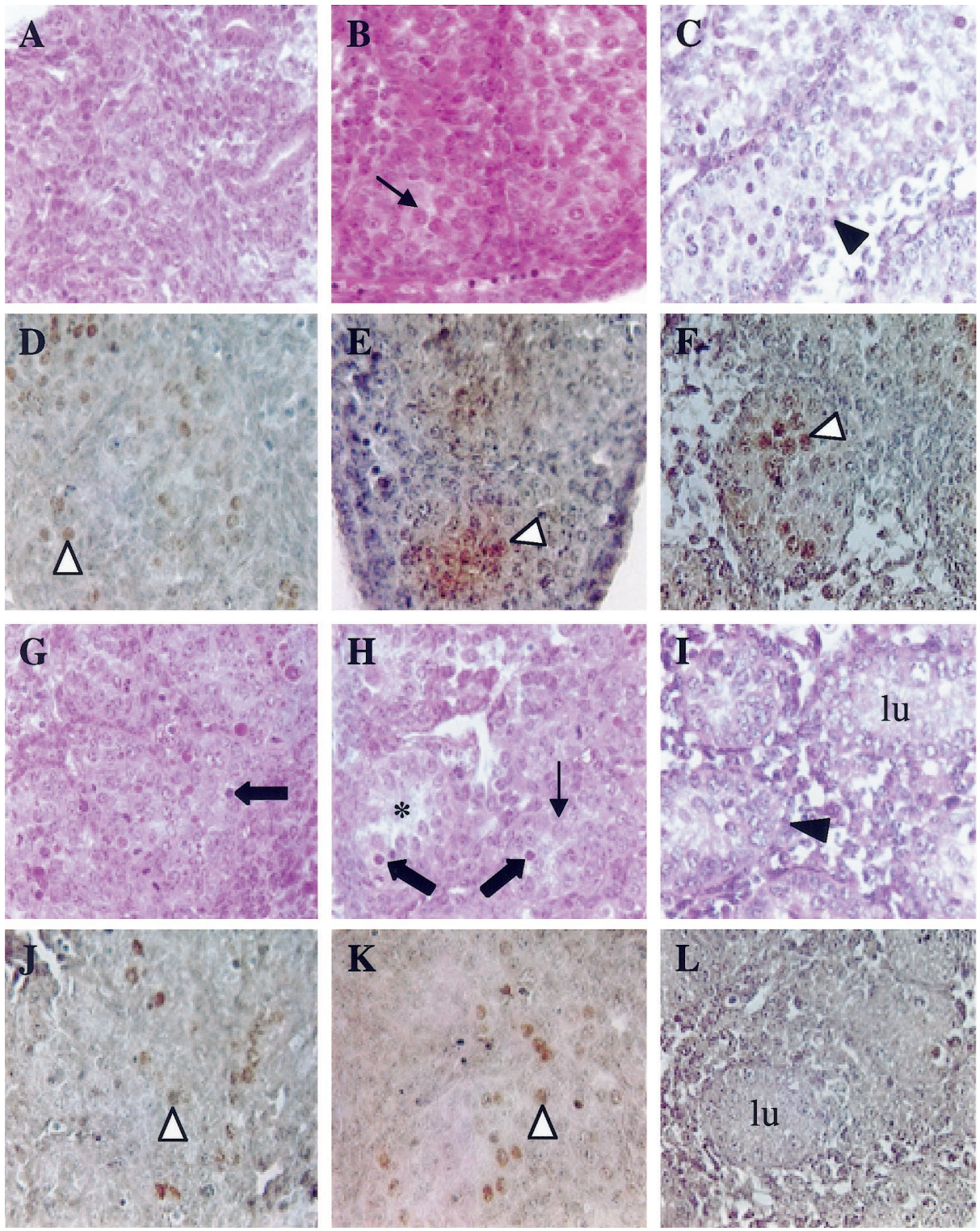

Fig. 4. The Loss of Gonocytes in fl^{neo}/fl^{neo} Embryos Occurs in the Embryonic Testis after Colonization by the Primordial Germ Cells

Testes from wild-type (A–F) and fl^{neo}/fl^{neo} embryos (G–L) were compared by H&E staining (A–C, G–I) and GCNA IHC (D–F, J–L) at different developmental stages. Germ cells are found in E12.5 (A and D) and E13.5 (B and E) control testes as well as E12.5 (G and J) and E13.5 (H and K) fl^{neo}/fl^{neo} testes. At E14.5, mutant testes (I and L) show a depletion in gonocytes compared with controls (C and F) within the developing seminiferous tubules. lu, Lumen; *arrowhead*, seminal cord; *white arrowhead,* GCNA-positive cells; *arrow*, normal gonocyte; *large arrow*, apoptotic cell; *asterisk*, developing lumen from loss of gonocytes. Original magnification is 630×.

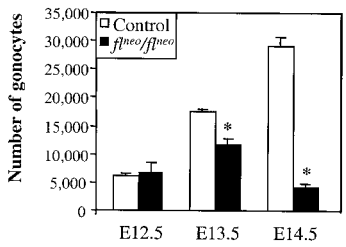

Fig. 5. Graphic Depiction of Gonocyte Numbers in *bcl-x* fl^{neo}/fl^{neo} and Wild-Type Fetal Gonads

Gonocyte numbers in wild-type and *bcl-x* fl^{neo}/fl^{neo} and testes between E12.5 and E14.5. Data represents the mean ± SEM. n = 3 for all samples.

range, 10.9%–22.9%) *vs.* control (4.5% ± 1.8; range, 2.5%–6.7%) (Fig. 4G). Even though both fl^{neo}/fl^{neo} and wild-type ovaries contained apoptotic germ cells, the fl^{neo}/fl^{neo} ovaries had a greater percentage of gonocytes undergoing apoptosis than the wild-type ovaries. At E13.5, the percentage of apoptotic gonocytes ranged from 28%–42.7% in the fl^{neo}/fl^{neo} ovaries, whereas it only ranged from 11.1%–19.1% in the wild-type ovaries (data not shown).

Transcriptional Initiation Sites in the *bcl-x* Gene and Expression of Bcl-x in Gonads

The *neo* gene was integrated 488 bp 5′ of the previously identified transcriptional start sites in the *bcl-x* gene (Fig. 7) (24). To test whether the tissue-specific hypomorphic allele was the result of more distal transcription start sites in gonads that are juxtaposed to the neo gene, we performed 5′-RACE (rapid amplification of cDNA ends) to identify *bcl-x* mRNA start sites in gonads. After having sequenced the products, we identified two additional *bcl-x* transcripts in the adult testis, ovary, and fetal gonad at −168 and −314 relative to the published start site. These sites were more distal from those previously reported in brain (+1) and thymus (+73) (Fig. 7). Transcriptional start sites in the adult and fetal gonads were confirmed by RT-PCR (data not shown).

To demonstrate that the loss of germ cells is attributed to a temporal specific down-regulation of the *bcl-x* gene, quantitative RT-PCR using TaqMan (Perkin-Elmer Corp., Norwalk, CT) was performed to obtain a relative expression profile of *bcl-x* to an endogenous control, glyceraldehyde 3-phosphate dehydrogenase (GAPDH). Approximately 150 germ cells were isolated from E12.5 gonads, and mRNA from lysed cells was used directly for cDNA synthesis. The first strand synthesis product was then used for quantitative RT-PCR analysis. Normalization of *bcl-x* mRNA obtained from germ cells was performed by comparison to GAPDH mRNA. Based on this internal standardization, there was an approximate 15-fold decrease in relative levels of *bcl-x* transcript in the gonocytes isolated from fl^{neo}/fl^{neo} gonads compared with control gonads (n = 4).

Ribonuclease (RNase) protection assays (RPAs) revealed a decline of *bcl-x* and other *bcl-2* family members from mRNA isolated from fl^{neo}/fl^{neo} (Fig. 8, lane 10) as compared with control (Fig. 8, lanes 7–9) testes, with the caveat that the mutant testes lacked spermatogonial cells. Bcl-w expression was not reduced in fl^{neo}/fl^{neo} testes, probably due to its localization also in Sertoli cells (16, 17). Variability of Bcl-w expression was found in wild-type controls (compare lanes 7–9). RPAs showed that the inserted *neo* gene had no effect on *bcl-x* gene expression in a variety of tissues from adult mice, including heart, kidney, and seminal vesicles (Fig. 8). Additional, nonreproductive tissues (*e.g.* brain, lung, and spleen) did not demonstrate a reduction in *bcl-x* message (data not shown). Histological examination of spleen, thymus, and liver in these mice did not reveal any differences compared with controls (not shown).

Expression of Bcl-x and Bax in the Fetal Testis

Bcl-x IHC established its expression at E13.5, the time when gonocytes are lost in fl^{neo}/fl^{neo} testis (Fig. 9). Expression in wild-type testes was confined to the PGCs (Fig. 9B), and expression was reduced in E13.5 fl^{neo}/fl^{neo} testis (Fig. 9A). Similarly, whole mount *in situ* hybridization demonstrated lower Bcl-x expression in fl^{neo}/fl^{neo} seminiferous tubules (data not shown). The loss of germ cells in fl^{neo}/fl^{neo} testes due to apoptosis was first observed at E13.5. To determine whether Bax could be a controlling factor in the apoptotic event, we performed IHC and established the expression of Bax at E13.5 (Fig. 9). Bax was expressed in wild-type testes at E13.5 and E14.5 in PGCs and, to a lesser degree, in somatic cells of the mesonephros (Fig. 9, D and E). The same staining pattern was observed in E13.5 fl^{neo}/fl^{neo} testes (Fig. 9C). No Bax expression was observed in wild-type testes at day E15.5. The Bax negative control (*bax*-null E14.5 testis) showed a low level of nonspecific product primarily restricted to the interstitial cells (Fig. 9F). RT-PCR confirmed that Bax is expressed in wild-type and fl^{neo}/fl^{neo} germ cells (Fig. 9G).

Genetic Rescue of the Loss-of-Germ-Cell Phenotype through the Deletion of Bax

Since Bax is expressed in PGCs, we investigated whether Bax induced the apoptosis and attrition of PGCs in fl^{neo}/fl^{neo} gonads. *Bax*-null alleles were bred into the *bcl-x* hypomorph [*bcl-x* fl^{neo}/fl^{neo}] to generate *bax*-null *bcl-x* hypomorph [*bax* −/−; *bcl-x* fl^{neo}/fl^{neo}] mice. The complete loss of Bax rescued the hypomorph loss-of-germ-cell phenotype as postnatal testes contain germ cells. At p1, *bax*-null *bcl-x* hypomorph testes (n = 3) had a 22-fold increase in the number of GCNA-positive cells per seminiferous tubule compared with the *bcl-x* hypomorph (n = 3) testis (Fig. 10B). GCNA IHC also showed the population of seminiferous tubules with germ cells in the *bax*-null

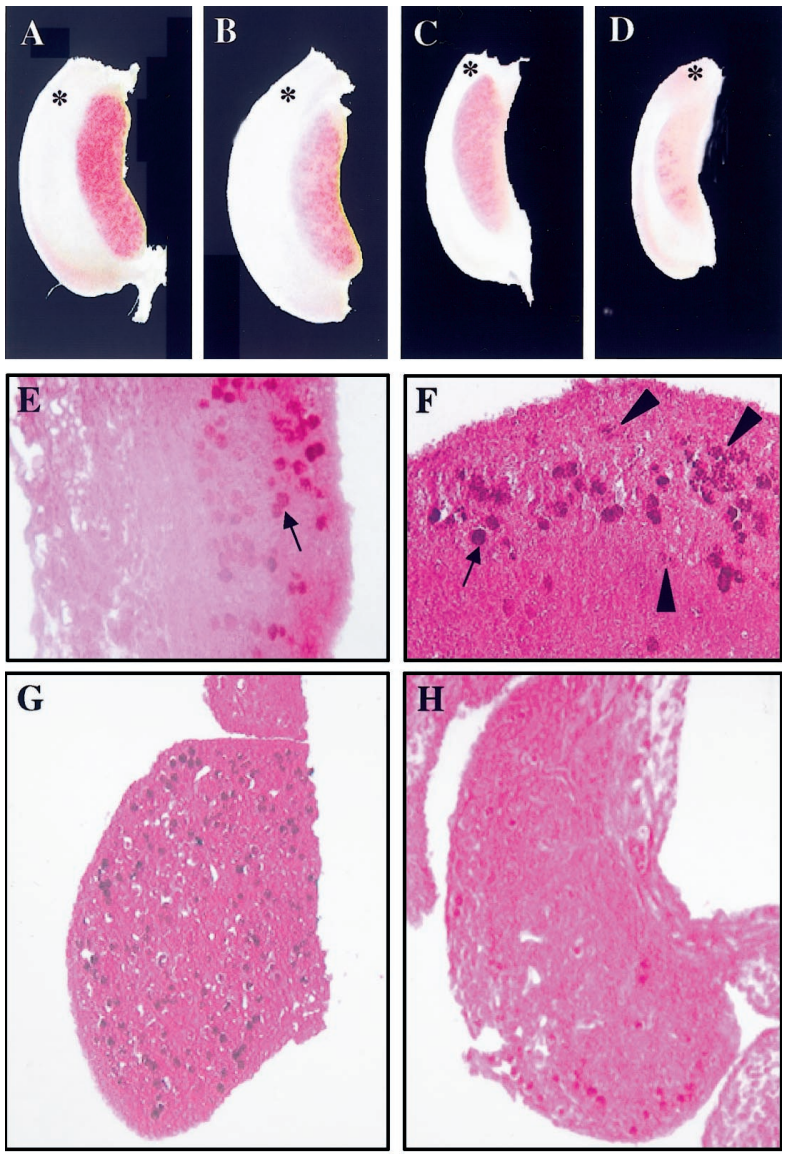

Fig. 6. Oocytes in fl^{neo}/fl^{neo} and Wild-Type Fetal Ovaries

AP levels were determined in mutant E13.5 (B) and E14.5 (D) ovaries and same stage controls at E13.5 (A) and E14.5 (C) as described in *Materials and Methods*. Visualization of germ cells in E14.5 control (E), E14.5 fl^{neo}/fl^{neo} (F), E15.5 control (G), and fl^{neo}/fl^{neo} ovaries (H), as determined by GCNA staining. *Arrow*, Normal germ cell; *arrowhead*, apoptotic germ cell; *asterisk*, mesonephros. Original magnification is 100× (A–D), 200× (G and H), 630× (E and F).

bcl-x hypomorph testes (n = 3) testis (Fig. 11). At p22, control testes (Fig. 12, A and B) showed spermatogonial descendants within the *bax* +/− and *bax* −/− seminiferous tubules. However, *bax* +/−; fl^{neo}/fl^{neo} (Fig. 12C) males did not have spermatogonia and *bax*-null *bcl-x* hypomorph testes (Fig. 12D) males had excess numbers of spermatogonia and spermatocytes resembling the *bax* −/− phenotype (14). Consistent with this, the *bax*-null *bcl-x* hypomorph and *bax*-null males were sterile (n > 6). Likewise, removal of both *bax* alleles from *bcl-x* hypomorph females resulted in higher follicle numbers compared with the *bcl-x* hypomorph females. At p1, there is a 4-fold increase in the number of follicles in *bax*-null *bcl-x* hypomorph ovaries *vs. bcl-x* hypomorph (n > 4) (Fig. 10A). Follicle counts in *bax*-null *bcl-x* hypomorph ovaries were actually higher than control ovary at the same stage. These females (n = 6) also had a normal reproductive lifespan and litter sizes that varied between 8–12 pups.

DISCUSSION

During embryonic life, germ cells migrate through the dorsal mesentery of the hindgut and arrive at the genital ridge around E11.5 to colonize the indifferent gonad (1, 2). In the male and female, mitotically active

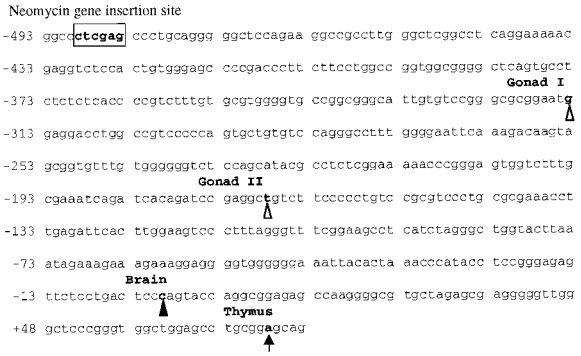

Fig. 7. 5′-RACE Shows That Gonads Have Additional Upstream Initiation Sites for mRNA Transcription of the bcl-x Gene

Bold, boxed sequence denotes the *Xho*I site into which the *neo* gene was cloned. *Bold bases* designate the transcription start sites for testis (two sites; determined in this study), brain (24), or thymus (24). *White arrowheads*, Gonad I and gonad II sites; *solid arrowhead*, brain site; *arrow*, thymus site. The numbering of the transcription start sites for bcl-x is relative to the initiation site in brain at (+1) (24). GenBank accession number AF088904.

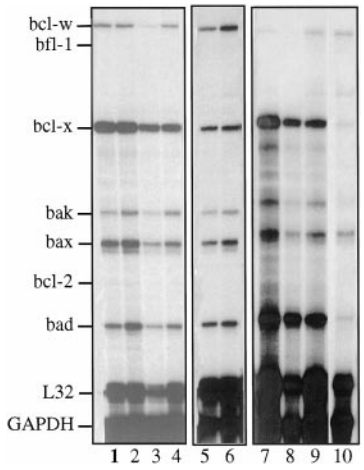

Fig. 8. RPA Shows That the Loss of *bcl-x* Is Tissue Specific

Total RNA was isolated from fresh mouse tissues by a modified guanidinium thiocyanate-phenol-chloroform procedure (48). Purified RNA (10 μg) was used with the m-Apo2 riboprobe template set (PharMingen, San Diego, CA) according to manufacturer's specifications with ^{32}P-UTP labeling (Amersham Pharmacia Biotech, Arlington Heights, IL). L32 and GAPDH were included as internal controls. Protected fragments were resolved using 6% polyacrylamide gels from Long Ranger gel solutions (J.T. Baker) at 120 V for 2 h in 0.5 × TBE. Lane 1, Wild-type heart; lane 2, fl^{neo}/fl^{neo} heart; lane 3, wild-type kidney; lane 4, fl^{neo}/fl^{neo} kidney; lane 5, wild-type seminal vesicle; lane 6, fl^{neo}/fl^{neo} seminal vesicle; lanes 7–9, wild-type testis; lane 10, fl^{neo}/fl^{neo} testis. mRNA was harvested from adult males approximately 3 months of age. Note that *bcl-x* is reduced in the mutant testis sample (lane 10) in comparison to control testis (lanes 7–9). Expression in the seminal vesicle remains equivalent between control (lane 5) and mutant (lane 6). Nonreproductive tissues similarly reflected endogenous expression profiles of *bcl-x* in mutant mice.

germ cells become quiescent at E15.5 and E13.5, respectively, with female germ cells immediately entering meiosis (5, 6, 25). Coincident with the loss of mitotic activity, many germ cells undergo attrition through apoptosis, which is suggested to be necessary for the future maintenance of supportive cells and germ cells in a distinct ratio (4). We now demonstrate that accurate regulation of Bcl-x concentration in PGCs is required for their survival during normal fetal gonad development, and that Bax is a counterbalance in this developmental process. This finding proves the concept that the balance of different Bcl-2 family members can determine cell survival and death *in vivo* (26).

A priori, cell survival imposed by Bcl-x should affect male and female germ cells similarly as determined by the levels of apoptosis. However, given the discrepancy between germ cell attrition in males and females in the *bcl-x* hypomorph, it is apparent that germ cell survival in the embryonic testis is more dependent upon Bcl-x. At p1, germ cells in the fl^{neo}/fl^{neo} male are decreased to 4% compared with wild-type, whereas female germ cells have declined to 34% of controls. Since female germ cells exit the mitotic cell cycle and enter meiosis about 1 day earlier than male germ cells, it is possible that the population of female germ cells that enter meiosis early are the ones that survive. The presence of a small percentage of oocytes after birth suggests that Bcl-x is important, but not essential, for female germ cell survival. Based on the presence of additional *bcl-x* transcripts with more distal start sites in germ cells, the *bcl-x* gene expression might be influenced by the presence of the *neo* gene at postnatal stages of development. This hypothesis is supported by comparison of follicle numbers in fl^{neo}/fl^{neo} and control ovaries at p1, p19, and 3 months. At p1, there is a 3-fold reduction in follicle numbers in fl^{neo}/fl^{neo} *vs.* control ovaries, compared with a 15-fold reduction in follicle numbers at p19. Likewise, there is a decrease in the primary and preantral follicle populations between p19 and 3 months in the fl^{neo}/fl^{neo} ovaries compared with control ovaries. The increased atresia in this model compliments the reduced atresia and increased reproductive lifespan found with *bax*-null females (15).

The *bcl-x* Hypomorph

The insertion of the *neo* gene in the promoter of the *bcl-x* gene resulted in a hypomorph allele that linked Bcl-x to germ cell survival. Although the time and effort is more considerable in pursuing the conditional gene targeting approach, the wealth of information from generating multiple alleles outweighs this concern. The altered alleles might display an altered expression profile and/or transcript that could lead to an analyzable phenotype (27, 28). Therefore, a single targeting event can be used to examine a combination of subtle

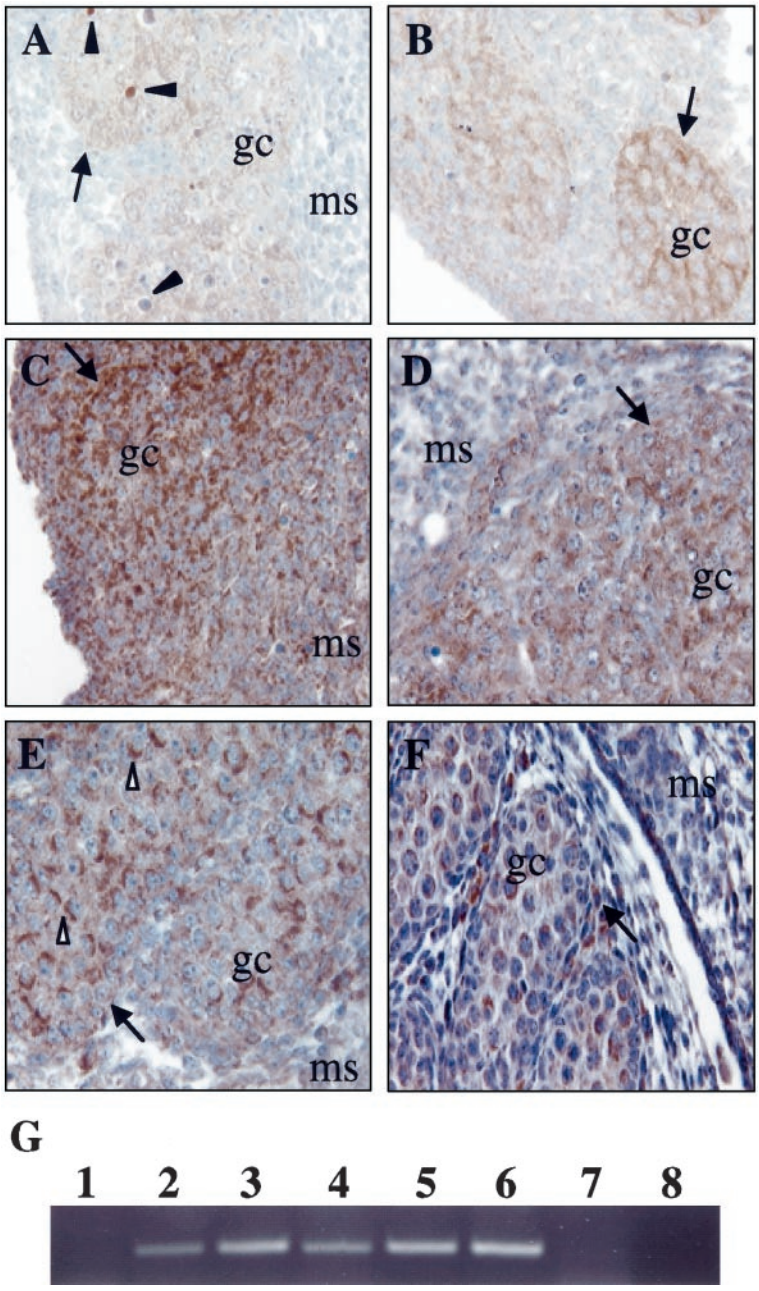

Fig. 9. IHC Localization of Bcl-x and Bax in Wild-Type and fl^{neo}/fl^{neo} Fetal Testes

Bcl-x was localized in E13.5 fetal testes as described in *Materials and Methods*. Panels A and B show Bcl-x staining in E13.5 seminiferous cords of fl^{neo}/fl^{neo} (A) and wild-type (B) mice. *Arrow*, Seminiferous cord; gc, germ cells; ms, mesonephros; *arrowhead*, apoptotic cells. Bax was localized in E13.5–15.5 fetal testes as described in *Materials and Methods*. Panels C and D show Bax staining in E13.5 seminiferous cords of fl^{neo}/fl^{neo} (C) and wild-type (D) mice. Panels E and F show Bax staining in E14.5 wild-type (E) and E14.5 *bax*-null (F) testes. *Arrow*, Seminiferous cord; gc, germ cells; ms, mesonephros; *arrowhead*, apoptotic cells; *white arrowhead*, Bax peri-nuclear staining. Original magnification is 630×. G, RT-PCR of *bax* expression in fetal testes. Lane 1, No DNA control; lanes 2–4, wild-type testes; lanes 5–6, fl^{neo}/fl^{neo} testes; lanes 7–8, *bax* −/− testes.

and complex phenotypes in the mouse. We have used this approach to demonstrate the role of Bcl-x in the ontogeny of germ cell development. We suggest that the tissue specificity of the *bcl-x* hypomorph allele is a result of cloning the *neo* gene within 170 bp to newly discovered, gonad-specific transcriptional start sites in the *bcl-x* gene promoter. Reversal of the phenotype upon removal of the *neo* gene also demonstrated that the remaining loxP site is not embedded within a critical *cis* element. Bcl-x IHC, TaqMan quantitative RT-PCR, and *in situ* hybridization demonstrate that there is a reduction of Bcl-x protein and mRNA in fl^{neo}/fl^{neo}

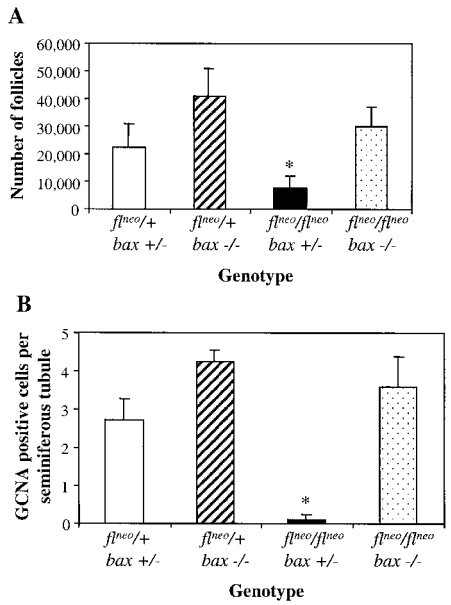

Fig. 10. Graphical Depiction of Germ Cell Numbers in p1 Gonads

Gonads were obtained from *bax* hemizygous or homozygous-null mice containing 1 or 2 hypomorphic *bcl-x* alleles. Gonads were collected and counted from female (A) and male (B) mice. For testes, n = 3; for ovaries, n = 9 for $fl^{neo}/+$; *bax* +/−; n = 7 for $fl^{neo}/+$; *bax*−/−; n = 5 for fl^{neo}/fl^{neo}; *bax* +/− and fl^{neo}/fl^{neo}; *bax*−−/−. For ovaries, $P = 0.03$ for fl^{neo}/fl^{neo}; *bax* +/− *vs.* $fl^{neo}/+$; *bax* +/− and $P < 0.003$ for fl^{neo}/fl^{neo}; *bax* +/− *vs*. $fl^{neo}/+$; *bax*−/− and fl^{neo}/fl^{neo}; *bax* −/−. For testes, $P < 0.003$.

fetal gonads compared with wild-type fetal gonads. The RPA validated the tissue specificity of the hypomorph, as *bcl-x* mRNA levels are equivalent in other fl^{neo}/fl^{neo} and wild-type tissues examined. We suggest that the neo gene located in the *bcl-x* promoter prevents the full utilization of transcriptional elements required for a normal developmental expression profile in the fetal gonads.

The common biological theme in cell development and maturation is that the loss of a proapoptotic factor leads to a decrease in apoptosis, whereas the elimination of an antiapoptotic factor results in increased apoptosis (26, 29). The role of four proteins from the Bcl-2 family (Bcl-x, Bax, Bcl-2, Bcl-w) in gonadal development has now been addressed through gene deletion. Their essential functions appear to be stage specific and nonoverlapping. *Bcl-2* null mice have a statistically significant reduced number of primordial follicles and diminished levels of primary and preantral stage follicles (11). Bax has been implicated in granulosa cell death, as ovaries of *bax*-null mice have fewer atretic cells in atretic follicles (14). *Bax* −/− and *bcl-w* −/− males are both infertile and do not produce mature sperm. Germ cells in *bcl-w* −/− males are generally depleted by 6 months of age with subsequent reduction in the Sertoli cell and Leydig cell populations (16, 17). While Bax, Bcl-w, and Bcl-2 have been shown to preferentially control postnatal stages of germ cell development and maturation, Bcl-x is required at a very early stage, providing for germ cell survival in the fetal gonad (Fig. 13). The *bcl-x* gene encodes two alternatively spliced transcripts (30), one encoding a cell survival molecule (Bcl-x_L) and one encoding a protein (Bcl-x_S) that can induce cell death *in vitro* (31). Suppression of bcl-x transcripts in our hypomorph would affect both splice forms. However, since *bcl-*x_S mRNA is far less abundant than *bcl-*x_L mRNA and can only be detected by RT-PCR (32, 33), its role *in vivo* remains unknown.

The *Bcl-x*/*Bax* Rheostat

Based on our results, we propose a genetic mechanism controlling the balance of germ cell survival and the surge of apoptosis during fetal development where Bcl-x and Bax are competing factors in this determination. A Bcl-x/Bax rheostat model is in accord with a Bcl-2/Bax rheostat model proposed by Korsmeyer and co-workers (34). Although the rheostat model implies a direct interaction between Bcl-x and Bax to elicit the cellular response, either heterodimerization-dependent or -independent mechanisms for these molecules could occur. Survival and death *in vivo* through the balance of Bcl-x and Bax probably contains cell-specific components since the absence of Bax can rescue germ cells (this study) as well as neurons, but not hematopoietic cells in *bcl-x*/*bax*-deficient embryos (35). We suggest that the decline of Bcl-x during gonad development in the *bcl-x* hypomorph allows Bax to proceed unabated in promoting cell death, as Bax is clearly present in the time window of the apoptotic surge between E12.5 and E14.5. Removal of both *bax* alleles from the *bcl-x* hypomorph restores the survival of germ cells, further demonstrating that the ratio of Bax and Bcl-x in the developing PGCs is critical for the demarcation and regulation of pathways for cell survival and cell death. Bcl-x_L can inhibit PGCs from undergoing apoptosis *in vitro* (36).

The Bcl-x/Bax rheostat model has also been demonstrated to define cell fate in yeast as well as mammalian cells. Expression of Bax in *Saccharomyces pombe* (37) or *Saccharomyces cerevisiae* (38) leads to cell death. However, coexpression of Bax and Bcl-x resulted in a suppression of apoptosis. Human polymorphonuclear neutrophils have been shown to decrease *bcl-x* mRNA upon induction of apoptosis or decrease *bax* mRNA in response to apoptotic inhibitors (39). The Bcl-x/Bax ratio might also be an important indicator in α_1-adrenoceptor activation, which increases myocardial resistance to ischemic injury, thereby reducing cell death (40). Ovarian follicle development is also linked to maintenance of this ratio. Follicle growth and survival in the rat are correlated with an attenuation of *bax* mRNA while *bcl-2* and *bcl-x* mRNAs are relatively constant. *In vitro* induction of apoptosis in antral staged follicles was associated with a decrease in Bcl-x and an increase in Bax (41). Our genetic studies now support these correlative studies on the Bcl-x/Bax rheostat.

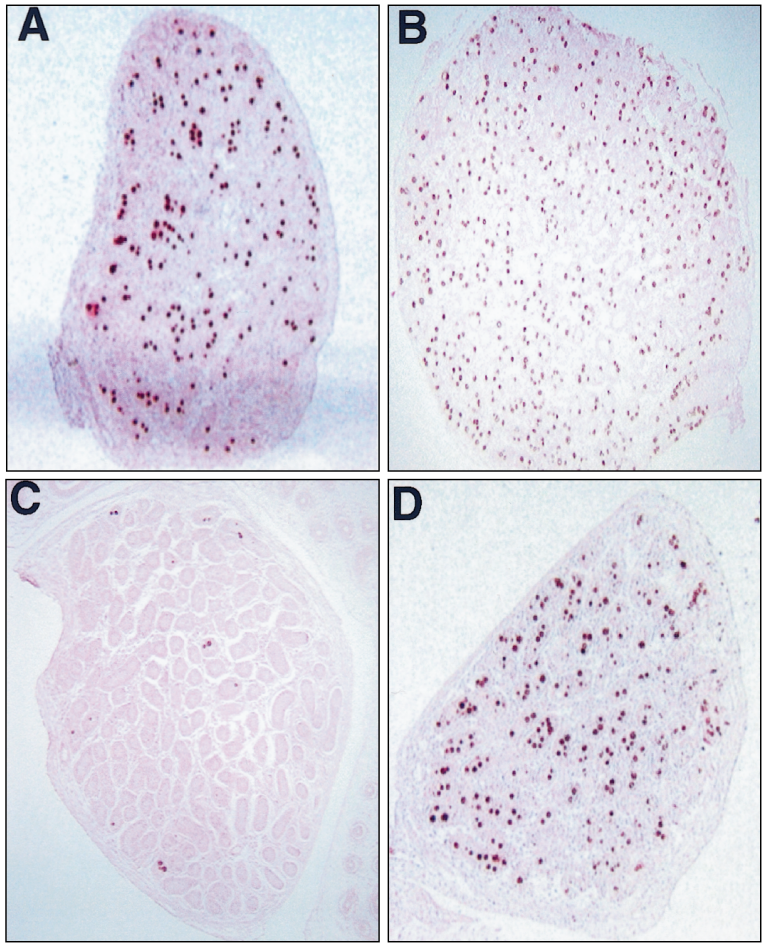

Fig. 11. Rescue of the *bcl-x* Hypomorph Male Phenotype through the Deletion of Bax

Cross-sections of p1 testes of (A) *bcl-x* $fl^{neo}/+$*; bax* $+/-$, (B) *bcl-x* $fl^{neo}/+$*; bax* $-/-$, (C) *bcl-x* fl^{neo}/fl^{neo}*; bax* $+/-$ and (D) *bcl-x* fl^{neo}/fl^{neo}; *bax* $-/-$ mice. Removal of one *bax* allele did not reverse the *bcl-x* hypomorph phenotype, whereas the loss of both *bax* alleles resulted in an increase in germ cells in the testis. GCNA IHC was performed on all testes with eosin counterstaining. Original magnification is 100×. HistoBank accession numbers 1354, 1355, 1356, 1357.

The Bcl-2 Family in Germ Cell Development

Several Bcl-2 family members (Bax, Bcl-2, Bcl-w) have been linked to germ cell development through gene deletion experiments (Fig. 13) (11, 14, 16, 17). Gametogenesis requires a balance of these members, although spermatogenesis appears to be less refractory to their altered expression than does folliculogenesis. Generally, gene disruption (Bcl-w, Bax) leads to male sterility at postnatal stages of development. In the ovary, removal of Bax or Bcl-2 leads to a surfeit or reduction in the number of primordial follicles, respectively (11, 14); however, neither *bax*-null nor *bcl-2*-null females are sterile. Bax is important for ovarian function as *bax*-deficient females contain an excess of primordial follicles during postnatal life and exhibit a prolonged ovarian life span into advanced chronological age (15). Likewise, the balance of these members has been shown to be important because ectopic expression of Bcl-x and Bcl-2 in the germ cells under the PGK promoter leads to male sterility (9). However, Bcl-x appears to be more important than Bcl-2 during spermatogenesis since Bcl-2 is expressed at very low levels in normal mouse testis. While Bax, Bcl-w, and Bcl-2 have been shown to control preferentially postnatal stages of germ cell development and maturation, Bcl-x is required at an early stage for germ cell survival in the fetal gonad. The availability of the *bcl-x* hypomorph in combination with the *bax*-null mice has now established a balancing role for these molecules in fetal germ cell development. Whether Bcl-x, like Bax, also modulates postnatal gametogenesis remains unknown and awaits the conditional inactivation of the floxed *bcl-x* gene at distinct stages of development using current Cre transgenic mice.

MATERIALS AND METHODS

Construction of the *bcl-x* Targeting Plasmid

A 10.5-kb *Eco*RV fragment of the *bcl-x* gene was isolated from a mouse 129/SvJ λ genomic DNA library clone and ligated into Bluescript IISK (pBS, Stratagene, La Jolla, CA). This clone contained 3.5 kb of the promoter, exon 1, intron 1,

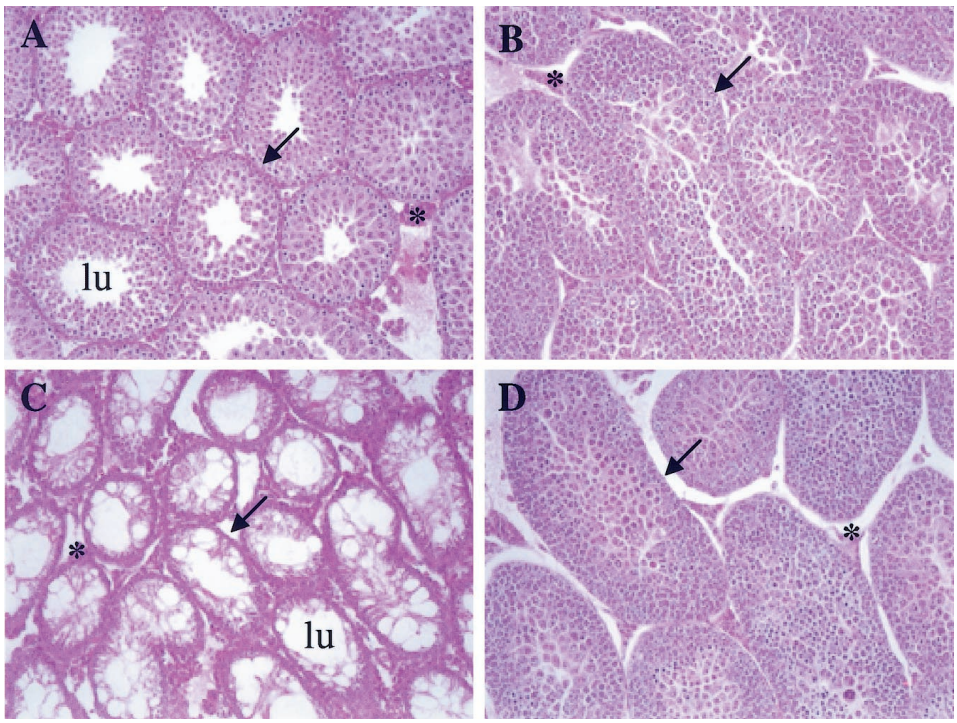

Fig. 12. Dominance of the *bax*-Null Phenotype over the *bcl-x* Hypomorph

Cross-sections of seminiferous tubules from p22 testes of *bax* +/− (A) and *bax* −/− (B) mice. C, Removal of one *bax* allele in *bax* −/+; *bcl-x* fl^{neo}/fl^{neo} mice did not reverse the loss-of-germ-cell phenotype. D, The loss of both *bax* alleles results in the presence of spermatogenesis in *bax* −/−;*bcl-x* fl^{neo}/fl^{neo} testis. H&E staining was performed on all sections. lu, Lumen; *, Leydig cells; *arrow,* seminiferous tubule. Original magnification is 200×.

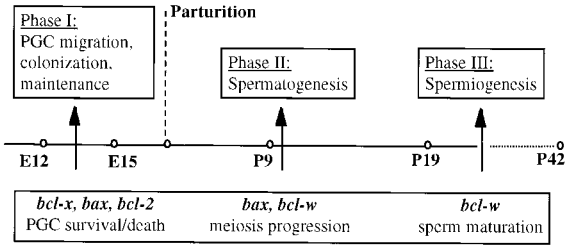

Fig. 13. Schematic Depicting Proposed Roles of Bcl-2 Family Members in Germ Cell Survival and Apoptosis

The timeline above represents both embryonic (E) and postnatal (P) stages of growth, in days.

exon 2, and 5.5 kb of intron 2. The targeting construct pBXFL was prepared by cloning a floxed neo gene into the *Xho* site in the promoter, a downstream loxP site within intron 2 at the *Spe*I site, and a thymidine kinase (TK) gene at the *bcl-x*-pBS junction. The loxP site was generated by annealing two primers to give *Spe*I overhangs: 5′-CTA GAT AAC TTC GTA TAA TGT ATG CTA TAC GAA GTT AT-3′ and 5′-CTA GAT AAC TTC GTA TAG CAT ACA TTA TAC GAA GTT AT-3′. Both the neo and TK genes were regulated by the PGK-I promoter and polyadenylation signal and were obtained from plasmid pPNT (42). The TK cassette was used to enrich for colonies that had undergone homologous recombination *vs.* random integration. The floxed neomycin plasmid pNeop was prepared by ligating a Klenow filled-in *Xho*I-BamHI fragment from pPNT into a *Bam*HI digested and Klenow filled-in double loxP plasmid pBS246 (Life Technologies, Inc., Gaithersburg, MD). An *Eco*RI–*Not*I fragment from pNeop was Klenow filled-in and ligated into a filled-in *Xho*I site of the *bcl-x*/*loxP* plasmid to generate plasmid pNpbx. For cloning of the TK cassette, a *Not*I–*Sma*I–*Sgf*I linker was introduced into the *Not*I site of the *Eco*RV–*Eco*RV bcl-x clone using the following oligonucleotides: 5′-GGC CGC GCC CGG GCG CGA ATC GCA T-3′; 5′-GGC CAT GCG ATC GCG CCC GGG CGC-3′. The TK cassette was directionally cloned into pNpbx as an *Sgf*I-*Not*I fragment from pBS-TK; pBS-TK contained an engineered *Sgf*I site at the *Sal*I site and the *Bam*HI-*Hin*dIII TK fragment from pPNT. The functionality of the loxP sites was determined before electroporation by transfecting pBXFL into bacterial AM-1 cells and by DNA sequencing (43).

Embryonic Stem (ES) Cell Targeting at the *bcl-x* Locus and Generation of fl^{neo} Mice

Linearized vector (25 μg) was electroporated (600 V/25 μFarads) into 2 × 10^7 TCI 129SvEv ES cells and maintained as described previously (44). Colonies resistant to G418 (280 μg/ml) and FIAU (0.2 μM) selection were isolated 7 days after electroporation. Clones verified as targeted by Southern hybridization were checked for the downstream loxP site by PCR using forward (5′-GCC ACC TCA TCA GTC GGG-3′) and reverse (5′-TCA GAA GCC GCA ATA TCC CC-3′) primer. The reaction conditions were 4 min at 94 C (1 cycle), 30 sec at 94 C/30 sec at 56 C/30 sec at 72 C (30 cycles), 5 min at 72 C. The endogenous allele gave a 160-bp band while the targeted allele was 195 bp in size. Positive ES cell clones were injected into 3.5-day blastocysts harvested from superovulated C57BL/6 donors (2.5 U PMSG, Calbiochem, La Jolla, CA ; 2.5U hCG, Organon, West Orange, NJ). Germline transmission was evaluated by backcrossing into a C57BL/6 background. Offspring carrying a floxed allele with a neo

Table 1. HistoBank Accession Numbers of High Resolution Images Presented in This Paper

Image	Histobank ID
Male reproductive organs (wild-type)	1456
Male reproductive organs (bcl-x fl^{neo}/fl^{neo})	1458
Male reproductive organs (bcl-x fl^{neo}/fl^{neo} and wild-type)	1457
Seminiferous tubules 3 month (wild-type) 200×	1363
Seminiferous tubules 3 month (bcl-x fl^{neo}/fl^{neo}) 200×	1362
Seminiferous tubules 3 month (bcl-x fl^{neo}/fl^{neo}) 630×	1342
Seminiferous tubules P19 (bcl-x fl^{neo}/fl^{neo}) 630×	371
Seminiferous tubules P19 (wild-type) 630×	370
Seminiferous tubules P22 (wild-type) 200×	1498
Seminiferous tubules P22 (bcl-x *fl*/-) 200×	1499
Testis P1 (wild-type) GCNA staining	1354
Testis P1 (bcl-x fl^{neo}/fl^{neo}; bax +/+) GCNA staining	1355
Testis P1 (bcl-x fl^{neo}/fl^{neo}; bax +/−) GCNA staining	1356
Testis P1 (bcl-x fl^{neo}/fl^{neo}; bax −/−) GCNA staining	1357
Ovary P9 (wild-type) 640×	1360
Ovary P9 (bcl-x fl^{neo}/fl^{neo}) 630×	1361
Ovary P19 (wild-type) 630×	1359
Ovary P19 (bcl-x fl^{neo}/fl^{neo}) 630×	1358
Ovary E13.5 (bcl-x fl^{neo}/fl^{neo} and wt) 200× (alk phosphatase)	1521
Ovary E13.5 (bcl-x fl^{neo}/fl^{neo}) Weigert's stain	1523
Ovary E13.5 (wild-type) Weigert's stain	1524

HistoBank is the repository for high-resolution histology images and was established at the National Institutes of Health. It can be accessed at http://HistoBank.nih.gov.

cassette were designated as fl^{neo} and represent a mixed C57BL/6–129SvEv background.

Generation and Genotyping of *bcl-x* Null (−), *bcl-x* Floxed (fl^{neo}), and *bax* Null Mice

Heterozygous bcl-x floxed mice ($fl^{neo}/+$) were mated with *MMTV-Cre* mice that exhibited Cre expression in the female germline (45). Cre transgenic $fl^{neo}/+$ dams were bred with wild-type males, and the progeny was checked for the recombined allele. Null alleles having a complete deletion of the floxed neomycin gene as well as exons 1 and 2 were confirmed by PCR. Reaction conditions were 4 min at 94 C (1 cycle), 30 sec at 94 C/30 sec at 58 C/30 sec at 72 C (30 cycles), 5 min at 72 C using forward (5′-CGG TTG CCT AGC AAC GGG GC-3′) and reverse primers (5′-TCA GAA GCC GCA ATA TCC CC-3′). The floxed neo cassette was deleted by crossing $fl^{neo}/+$ mice with *EIIa-Cre* mice (46). PCR reaction conditions were identical to the null allele verification using the following primers: forward, 5′-CGG TTG CCT AGC AAC GGG GC-3′; reverse, 5′ CTC CCA CAG TGG AGA CCT CG-3′. *Bax* knockout mice were a kind gift of Dr. Stanley Korsmeyer and were genotyped using the following primers and reaction conditions. For the wild-type allele, forward primer 5′-GTT GAC CAG AGT GGC GTA GG-3′ and reverse primer 5′-GAG CTG ATC AGA ACC ATC ATG-3′ were used under the same condition profile as described above. For the *bax* knockout allele, the same forward primer and PCR reaction profile as for the wild-type were used with a different reverse primer, 5′-CCG CTT CCA TTG CTC AGC GG-3′. The wild-type allele gave a 300-bp band while the *bax* knockout allele gave a 506-bp band.

Sequence Analysis of the *bcl-x* Promoter Region

A 9.5-kb *Xba*I–*Xba*I fragment was sequenced with the AmpliTaq Dye Terminator Cycle Sequencing Kits (Perkin-Elmer Corp., Branchburg, NJ) on an ABI Prism 310 Genetic Analyzer (ABI Advanced Biotechnologies, Inc., Columbia, MD). Subclones were generated to facilitate sequencing using M13 forward and reverse primers: a 4-kb *Xba*I–EcoRV fragment, 3.5-kb *Eco*RV–*Hin*dIII fragment, and 2-kb *Hin*dIII–*Spe*I fragment were subcloned into pBS. Additional oligonucleotide sequencing primers were designed using the MacVector 4.0 program and synthesized by Lofstrand Oligos (Gaithersburg, MD). Sequences were compiled using the Sequencher 3.0 program (Gene Codes Corp., Ann Arbor, MI). GenBank accession number AF088904.

5′-RACE for Determination of Testis-Specific Transcripts

One microgram of total RNA isolated from wild-type mouse testis was used for the 5′-RACE procedure (Life Technologies, Inc.) as described by the manufacturer. The *bcl-x*-specific primer 1 used for the first strand cDNA synthesis is as follows: 5′-TGT GTT TAG CGA TTC TC-3′. Amplification of the 5′-transcripts was performed using an abridged universal amplification primer (provided in kit) and a *bcl-x*-specific primer 2 (5′-TAA GGT TAT TCA AAT CTA TCT CC-3′). Amplification was performed using Platinum *Taq* (0.25U, Life Technologies, Inc.) under the standard conditions described in the kit. Amplicons were cloned into pCRII vector (Invitrogen, San Diego, CA) and sequenced using M13 forward and reverse primers.

Quantitation of *bcl-x* Expression Levels Using the TaqMan PCR System

Germ cells were isolated from appropriate staged embryos as previously described using an EDTA treatment protocol (47). Yolk sacs were collected for PCR verification of embryo genotype. Between 50 and 75 PGCs per gonad were transferred by mouth pipette into lysis buffer consisting of 1% NP-40, 6 mM dithiothreitol, and 10 U/μl of RNase inhibitor (Promega Corp., Madison, WI). SuperScript II first strand synthesis kit (Life Technologies, Inc.) with random primers was used to generate the template for PCR from the lysate. A 0.5-μl aliquot was used for PCR using the ABI Prism 7700 Sequence Detection system (ABI Advanced Biotechnologies, Inc.) and TaqMan PCR products (Perkin-Elmer Corp.). Primers and probe for the *bcl-x* amplification were generated using Primer Express (Perkin-Elmer Corp.): forward primer, 5′-ACC ACC TAG AGC CTT GGA TCC- 3′; reverse primer, 5′-TCT CGG CTG CTG CAT TGT T-3′; bcl-x probe, 5′-6-FAM ACG GCG GCT GGG ACA CTT TTG TG-TAMRA-3′. Reaction conditions consisted of 10 min at 95 C (1 cycle), 15 sec at 95 C/60 sec at 60 C (40 cycles) with 200 nM primers and probe. GAPDH and 18S control PCR kits were used to normalize expression levels. Data were exported into Microsoft Corp. Excel for analysis. Statistical significance was determined by the Whitney-Mann U test to be at the 98% confidence level.

GCNA, Bcl-x, Bax IHC, and Bax RT-PCR

Gonads were fixed in Bouin's solution (Sigma, St. Louis, MO) overnight, transferred to 70% ethanol, paraffin-embedded, and then sectioned at 5 μm. Sections were deparaffinized through ethanol, rehydrated in water, and placed in 0.03% (vol/vol) hy-

drogen peroxide in methanol for 30 min at room temperature. Sections were rinsed in 1× PBS, treated with 0.01 M citric acid, pH 6.0 at 90 C for 10 min, slow cooled an additional 10 min, and finally rinsed in 1× PBS. Blocking was performed with 10% serum at room temperature for 30 min followed by the addition of diluted GCNA antibody (1:2), Bcl-x antibody (1:50; Santa Cruz no. sc-1041; Santa Cruz Biotechnology, Inc., Santa Cruz, CA) or Bax antibody (1:50; Santa Cruz no. sc-526; Santa Cruz Biotechnology, Inc.) for overnight incubation at 4 C. Upon washing in 1× Tris-buffered saline (TBS), peroxidase-conjugated secondary antibody (1:300) was added for 1 h at room temperature. After rinsing in 1× TBS, samples were incubated in ABC solution and treated with 3′,3-diaminobenzidine (Vector Laboratories, Inc., Burlingame, CA) according to manufacturer's protocol). Slides were counterstained and mounted with Permount (Sigma). For RT-PCR, RNA was isolated from germ cells and used in a first-strand synthesis reaction as described in the previous section. Bax forward (5′-ATG CGT CCA CCA AGA AGC TGA G-3′) and reverse primers (5′-CCC CAG TTG AAG TTG CCA TCA G-3′) were used to amplify a 162-bp diagnostic band. Reaction conditions consisted of 30 μM of each primer in the following profile: 4 min at 94 C (1 cycle), 30 sec at 94 C/30 sec at 58 C/30 sec at 72 C (30 cycles), 5 min at 72 C.

AP Staining

Embryos were collected and fixed in absolute ethanol-glacial acetic acid (7:1) for 1 h at 4 C and replaced twice within 24 h with absolute ethanol as described previously (23). Samples were then placed in two changes of xylene after 12 h and rehydrated with two changes of absolute ethanol and one change of 70% ethanol for 1–2 h each. Using distilled water, embryos were rinsed three times, 10 min each, and transferred to freshly prepared AP stain for 15–20 min as monitored under a dissecting stereo microscope. AP aqueous staining solution contained 10 μg/ml α-naphthyl phosphate (Sigma), 0.5 mg/ml Fast Red TR (Sigma), 0.06% (wt/vol) $MgCl_2$, and 0.45% (wt/vol) Borax (Sigma). Color development was stopped by placing embryos in distilled water.

Histological Evaluation of Gonads

Gonads were fixed in Bouin's solution for 18–24 h and then washed with 70% ethanol. After fixation, the tissues were dehydrated, embedded in Paraplast (VWR Scientific,), serially sectioned (8 μm, ovaries; 5 μm, testes), mounted on glass slides, and stained with Weigert's hematoxylin-picric acid methylene blue (ovaries) or hematoxylin-eosin (testes). Counting was performed on every tenth section for embryonic and postnatal gonads. For ovaries, each section was qualitatively evaluated for the appearance of the ovarian follicles. Follicles were identified as normal if they contained an intact oocyte, organized granulosa and thecal cell layers, and no pyknotic bodies. Follicles were considered atretic if they contained either a degenerating oocyte, disorganized granulosa cells, pyknotic nuclei, shrunken granulosa cells, or apoptotic bodies. Apoptotic bodies were identified as bodies in the granulosa cell layers or PGCs that contained dark-staining masses of condensed chromatin.

Statistical Analysis

The mean number of germ cells or ovarian follicles was calculated using ovaries from at least three different animals. Differences in germ cell and follicles numbers were evaluated by one-way ANOVA, with statistical significance assigned at $P < 0.05$. When a significant P value was obtained, Scheffe's test was used in the post hoc analysis. The SPSS (version 10) program (SPSS, Inc., Chicago, IL) was used to compile statistics from the obtained data.

Acknowledgments

The authors wish to thank G. Enders for his kind gift of the GCNA antibody and constructive criticism of the manuscript, S. Korsmeyer for the bax-null mice, D. Loh and Nobura Motoyama for the bcl-x clone, H. Westphal for the EIIa-Cre transgenic mice, J. Babus for histology work, and K. Heermeier for the bcl-x subcloning. We are grateful to C. Deng, G. Robinson, N. Strunnikova, M. Gallego, J. Shillingford, and R. Humphreys for their technical advice and insight. We would like to thank Ulrike Wagner for her computational assistance with HistoBank.

Received July 26, 1999. Re-revision received February 16, 2000. Accepted February 21, 2000.

Address requests for reprints to: Lothar Hennighausen, Laboratory of Genetics and Physiology, 9000 Rockville Pike Bethesda, Maryland 20892. E-mail: mammary@nih.gov.

E.B.R. was supported by a NIH staff fellow award. Funds for the project were obtained from NIH intramural resources. K.U.W. was supported by a Deutsche Forschungsgemeinschaft fellowship (WA 1119/1–1).

* Current address: University of California San Diego School of Medicine, La Jolla, California 92093-0627.

REFERENCES

1. Eddy EM, Clark JM, Gong D, Fenderson BA 1981 Origin and migration of primordial germ cells in mammals. Gamete Res 4:333–362
2. Clark JM, Eddy EM 1975 Fine structural observations on the origin and association of primordial germ cells in the mouse. Dev Biol 47:136–155
3. Tam PPL, Snow MHL 1981 Proliferation and migration of primordial germ cells during compensatory growth in mouse embryos. J Embryol Exp Morphol 64:133–147
4. Coucouvanis EC, Sherwood SW, Carswell-Crumpton C, Spack EG, Jones PP 1993 Evidence that the mechanism of prenatal germ cell death in the mouse is apoptosis. Exp Cell Res 209:238–247
5. Peters H 1970 Migration of gonocytes into the mammalian gonad and their differentiation. Philos Trans R Soc Lond B Biol Sci 259:91–101
6. Borum K 1967 Oogenesis in the mouse. A study of the origin of the mature ova. Exp Cell Res 45:39–47
7. Nebel BR, Amarose AP, Hackett EM 1961 Calendar of gametogenic development in the prepuberal male mouse. Science 134:833–834
8. Mori C, Nakamura N, Dix DJ, Fujioka M, Nakagawa S, Shiota K, Eddy EM 1997 Morphological analysis of germ cell apoptosis during postnatal testis development in normal and Hsp 70–2 knockout mice. Dev Dyn 208: 125–136
9. Rodriguez I, Ody C, Araki K, Garcia I, Vassalli P 1997 An early and massive wave of germinal cell apoptosis is required for the development of functional spermatogenesis. EMBO J 16:2262–2270
10. Ratts VS, Flaws JA, Kolp K, Sorenson CM, Tilly JL 1995 Ablation of bcl-2 gene expression decreases the numbers and oocytes and primordial follicles established in the post-natal female mouse gonad. Endocrinology 136: 3665–3668
11. Wang RA, Nakane PK, Koji T 1998 Autonomous cell death of mouse male germ cells during fetal and postnatal period. Biol Reprod 58:1250–1256
12. Mintz B, Russell ES 1957 Gene-induced embryological modifications between stem cell factor and the colony stimulating factors. J Exp Zool 134:207–237

13. McCoshen JA, McCallion DJ 1975 A study of the primordial germ cells during their migratory phase in Steel mutant mice. Experientia 31:589–590
14. Knudson CM, Tung KS, Tourtellotte WG, Brown GA, Korsmeyer SJ 1995 Bax-deficient mice with lymphoid hyperplasia and male germ cell death. Science 270: 96–99
15. Perez GI, Robles R, Knudson CM, Flaws JA, Korsmeyer SJ, Tilly JL 1999 Prolongation of ovarian lifespan into advanced chronological age by Bax-deficiency. Nat Genet 21:200–203
16. Print CG, Loveland KL, Gibson L, Meehan T, Stylianou A, Wreford N, de Kretser D, Metcalf D, Kontgen F, Adams JM, Cory S 1998 Apoptosis regulator bcl-w is essential for spermatogenesis but appears otherwise redundant. Proc Natl Acad Sci USA 95:12424–12431
17. Ross AJ, Waymire KG, Moss JE, Parlow AF, Skinner MK, Russell LD, MacGregor GR 1998 Testicular degeneration in Bclw-deficient mice. Nat Genet 18:251–256
18. Gonzalez-Garcia M, Perez-Baluster R, Ding L, Buan L, Boise L, Thompson C, Nunez,G 1994 Bcl-X_L is the major bcl-X mRNA form expressed during murine development and its product localizes to mitochondria. Development 120:3033–3042
19. Motoyama N, Wang F, Roth KA, Sawa H, Nakayama K, Nakayama K, Negishi I, Senju S, Zhang Q, Fujii S, Loh D 1995 Massive cell death of immature hematopoietic cells and neurons in Bcl-x-deficient mice. Science 267: 1506–1510
20. Sternberg N, Hamilton D 1981 Bacteriophage P1 site-specific recombination. I. Recombination between loxP sites. J Mol Biol 150:467–486
21. Lakso M, Pichel JG, Gorman JR, Sauer B, Okamoto Y, Lee E, Alt FW, Westphal H 1996 Efficient *in vivo* manipulation of mouse genomic sequences at the zygote stage. Proc Natl Acad Sci USA 93:5860–5865
22. Enders GC, May JJ 2nd 1994 Developmentally regulated expression of a mouse germ cell nuclear antigen examined from embryonic day 11 to adult in male and female mice. Dev Biol 163:331–340
23. Ginsburg M, Snow MH, McLaren A 1990 Primordial germ cells in the mouse embryo during gastrulation. Development 110:521–528
24. Grillot DA, Gonzalez-Garcia M, Ekhterae D, Duan L, Inohara N, Ohta S, Seldin MF, Nunez G 1997 Genomic organization, promoter region analysis, and chromosome localization of the mouse bcl-x gene. J Immunol 158:4750–4757
25. Monk M, McLaren A 1981 X-chromosome activity in foetal germ cells of the mouse. J Embryol Exp Morphol 63:75–84
26. Oltvai ZN, Milliman CL, Korsmeyer SJ 1993 Bcl-2 heterodimerizes *in vivo* with a conserved homolog, Bax, that accelerates programmed cell death. Cell 74:609–619
27. Nagy A, Moens C, Ivanyi E, Pawling J, Gertsenstein M, Hadjantonakis AK, Pirity M, Rossant J 1998 Dissecting the role of N-myc in development using a single targeting vector to generate a series of alleles. Curr Biol 8:661–664
28. Meyers EN, Lewandoski M, Martin GR 1998 An Fgf8 mutant allelic series generated by Cre- and Flp-mediated recombination. Nat Genet 18:136–141
29. Adams JM, Cory S 1998 The Bcl-2 protein family: arbiters of cell survival. Science 281:1322–1326
30. Boise LH, Gonzalez-Garcia M, Postema CE,Ding L, Lindsten T,Turka LA, Mao X, Nunez G, Thompson CA 1993 Bcl-X, a bcl-2 related gene that functions as a dominant regulator of apoptotic cell death. Cell 74:597–608
31. Minn AJ, Boise LH, Thompson CB 1996 Bcl-x(S) antagonizes the protective effects of Bcl-x(L). J Biol Chem 271:6306–6312
32. Heermeier K, Benedict M, Li M, Furth P, Nunez G, Hennighausen L 1996 Bax and Bcl-xs are induced at the onset of apoptosis in involuting mammary epithelial cells. Mech Dev 56:197–207
33. Jurisicova A, Latham KE, Casper RF, Casper RF, Varmuza SL 1998 Expression and regulation of genes associated with cell death during murine preimplantation embryo development. Mol Reprod Dev 51:243–253
34. Korsmeyer SJ, Shutter JR, Veis DJ, Merry DE, Oltvai ZN 1993 Bcl-2/Bax: a rheostat that regulates an antioxidant pathway and cell death. Semin Cancer Biol 4:327–332
35. Shindler KS, Latham CB, Roth KA 1997 Bax deficiency prevents the increased cell death of immature neurons in bcl-x-deficient mice. J Neurosci 17:3112–3119
36. Watanabe M, Shirayoshi Y, Koshimizu U, Hashimoto S, Yonehara S Eguchi Y, Tsujimoto Y, Nakatsuji N 1997 Gene transfection of mouse primordial germ cells *in vitro* and analysis of their survival and growth control. Exp Cell Res 230:76–83
37. Jurgensmeier JM, Krajewski S,Armstrong RC, Wilson GM, Oltersdorf T, Fritz LC, Reed JC, Ottilie S 1997 Bax- and Bak-induced cell death in the fission yeast *Schizosaccharomyces pombe*. Mol Biol Cell 8:325–339
38. Greenhalf W, Stephan C, Chaudhuri B 1996 Role of mitochondria and C-terminal membrane anchor of Bcl-2 in Bax induced growth arrest and mortality in *Saccharomyces cerevisiae*. FEBS Lett 380:169–175
39. Weinmann P, Gaehtgens P, Walzog B 1999 Bcl-Xl- and Bax-α-mediated regulation of apoptosis of human neutrophils via caspase-3. Blood 93:3106–3115
40. Baghelai K, Graham LJ, Wechsler AS, Jakoi ER 1999 Delayed myocardial preconditioning by α1-adrenoceptors involves inhibition of apoptosis. J Thorac Cardiovasc Surg 117:980–986
41. Tilly JL, Tilly KI, Kenton ML, Johnson AL 1995 Expression of members of the bcl-2 gene family in the immature rat ovary: equine chorionic gonadotropin-mediated inhibition of granulosa cell apoptosis is associated with decreased bax and constitutive bcl-2 and bcl-xlong messenger ribonucleic acid levels. Endocrinology 136: 232–241
42. Tybulewicz VL, Crawford CE, Jackson PK, Bronson RT, Mulligan RC 1991 Neonatal lethality and lymphopenia in mice with a homozygous disruption of the c-abl proto-oncogene. Cell 65:1153–1163
43. Rucker EB, Piedrahita JA 1997 Cre-mediated recombination at the murine whey acidic protein (mWAP) locus. Mol Reprod Dev 48:324–331
44. Deng C, Wynshaw-Boris A, Kuo A, Zhou F, Leder P 1996 Fibroblast growth factor receptor-3 is a negative regulator of bone growth and development. Cell 84: 911–921
45. Wagner K-U, Wall RJ, St-Onge L, Gruss P, Garrett L, Wynshaw-Boris A, Li, M, Furth PA, Hennighausen L 1997 Cre mediated gene deletion in the mammary gland. Nucleic Acids Res 25:4323–4330
46. Lakso M, Pichel JG, Gorman JR, Sauer B, Okamoto Y, Lee E, Alt FW, Westphal H 1996 Efficient *in vivo* manipulation of mouse genomic sequences at the zygote stage. Proc Natl Acad Sci USA 93:5860–5865
47. Buehr M, McLaren A 1993 Isolation and culture of primordial germ cells. In: Methods in Enzymology. Academic Press, San Diego, CA, vol 225:58–77
48. Chomczynski P, Sacchi N 1987 Single step method of RNA isolation by acid guanidinium thiocyanate-phenol-chloroform extraction. Anal Biochem 162:156–159